Electric Taxiing with Disruption Management: Assignment of Electric Towing Vehicles to Aircraft

Zoutendijk, M.; van Oosterom, S.J.M.; Mitici, M.A.

DOI
10.2514/6.2023-4219

Publication date
2023

Document Version
Final published version

Published in
AIAA AVIATION 2023 Forum

AIAA AVIATION Forum
12-16 June 2023, San Diego, CA and Online
AIAA AVIATION 2023 Forum

10.2514/6.2023-4219

Electric Taxiing with Disruption Management: Assignment of Electric Towing Vehicles to Aircraft

Mike Zoutendijk* and Simon van Oosterom †
Delft University of Technology, Delft, 2629 HS, The Netherlands

Mihaela Mitici‡
Utrecht University, Utrecht, 3584 CS, The Netherlands

Reducing aircraft taxiing emissions will deliver a significant contribution to the worldwide goal of net-zero greenhouse gas emissions in the aviation industry. Replacing jet-engine taxiing by towing aircraft with electric towing vehicles is expected to reduce taxiing emissions by roughly 80%. Introducing a fleet of towing vehicles introduces operational challenges to an airport. Although there has been research focused on optimizing the assignment of vehicles to aircraft, such an assignment will require changes during a day of operations, when disruptions such as flight delays occur. This paper proposes two models, a strategic and a disrupted model, with which an adaptive vehicle-to-aircraft assignment is created. The models are formulated as Mixed Integer Linear Problems, and both maximize the number of towed aircraft and minimize the schedule changes for vehicle operators. The approach illustrated includes vehicle and aircraft routing, conflict avoidance, and a model for energy usage. We apply the models to Amsterdam Airport Schiphol, where the disrupted model is able to create assignments that remain the same in subsequent time steps for an average of 55% of the vehicles, on a busy day, when towing all aircraft. Furthermore, the results show that minimizing schedule changes does not come at the expense of fewer towed aircraft, i.e. of smaller emission savings. Lastly, we investigate the impact of fleet size and general on-time performance on the assignments created by the model.

I. Introduction

The aviation industry has the ambition of achieving net-zero greenhouse gas emissions before 2050 [1, 2]. An important part of total emissions is the ground-based emissions, created by activities on and around airports. Aircraft taxiing produces 54% of emissions related to the landing/take-off cycle [3], and is therefore a large contributor to ground-based emissions. A promising method to reduce taxiing emissions is to introduce a fleet of electric towing vehicles (ETVs) to airports, which tow the aircraft from gate to runway and vice versa. For example, research has shown that the use of ETVs will reduce the taxiing fuel use by roughly 80% [4, 5].

Implementing a fleet of ETVs on an airport brings about various challenges. In previous work, researchers have investigated the cost-effectiveness of ETVs [6, 7], their effect on on-time performance [8, 9], and they have modelled the expected decrease in fuel use, emissions and noise [9–12].

In addition, there are operational challenges, such as the assignment of vehicles to aircraft, the charging infrastructure and planning, the shared usage of airport roads, and the robustness of schedules under disruptions.

Vehicle-to-aircraft assignments Several models have been developed to generate vehicle-to-aircraft assignments for ETVs. For example, van Baaren and Roling [13] and Soltani et al. [14] created an LP model to select aircraft to be towed so that fuel reduction was maximized. The former performed a sensitivity analysis on ETV fleet size, while the latter included collision avoidance in their model. Ahmadi [15] created a complex LP model which minimized not only fuel reduction, but also ground delay costs and operating costs. van Oosterom et al. [16] created an MILP model minimizing the ETV fleet size. In a different approach, Zaninotto et al. [17] and Salihu et al. [18] performed the vehicle-to-aircraft assignment at the same time as the vehicle and aircraft routing, by simulating all ground movement and assigning the ETVs to aircraft that can reach them the first.

*PhD Candidate, Control & Operations, Kluyverweg 1 Delft
†PhD Candidate, Control & Operations, Kluyverweg 1 Delft
‡Assistant Professor, Information & Computing Sciences, Heidelberglaan 8 Utrecht

Energy model In order to obtain a realistic overview of airport surface movement in the situation of electric taxiing, it is essential to include the energy usage and vehicle recharging in the model. There are few studies which include airport surface movement planning, electric taxiing, and an energy model. One example is the model by van Baaren and Roling [13], which prescribes that every ETV is recharged to full capacity upon returning to the depot. Second, the model by van Oosterom et al. [16] includes three different charging strategies: night-charging, fixed-time charging and partial charging. They conclude that partial charging allows for the smallest ETV fleet size.

Disruption management After obtaining a model that takes into account all inputs and requirements and using it to generate a valid schedule, the schedule must be executed. During actual operations, disruptions to the schedule can occur that require airport planners to alter the schedule. We refer to this as *disruption management*. Questions pertaining to disruption management are:

- To what extent can the original schedule be used to obtain the disrupted schedule? What kind of changes to the schedules can be deployed?
- What metric is observed when changing the original schedule? What is the relation of this metric with the metrics observed when creating the original schedule?

An example of an application of disruption management in the aerospace domain is Lee et al. [19]. The authors formulate a Stochastic Mixed Integer Program to obtain a disrupted flight planning schedule for staggered time periods. The tools available to change the schedule include flying altitude and speed, and aircraft swaps and cancellations. Both real-time revealed disruptions and probabilistic forecasts of future disruptions are inputs to the model. The proposed model reduces the disruption recovery costs by 1 to 4% compared to a baseline flight planning model. In later work, the authors show that using probabilistic forecasts reduces expected recovery costs by 1 to 2% more than using only real-time disruptions [20].

To the best of our knowledge, there is no disruption management approach for assignment of electric towing vehicles to aircraft, or for general airport surface movement planning. In this paper we propose two MILP models specifically designed to facilitate disruption management for ETV-to-aircraft assignment at an operational level. The first model is a *strategic model*, which is used to obtain an initial vehicle-to-aircraft assignment for a four hour time window. The second model is a *disrupted model*, which is used to obtain a disrupted assignment, taking into account the effects of imminent flight delays, and minimizing the schedule changes from the perspective of ETV operators. This model is run at the start of staggered time periods. Airport layout information and flight schedules are used to obtain the routes for the aircraft and vehicles, after which they are used to generate vehicle-to-aircraft assignments. Realistic parameters and conditions are taken into account, such as the prevention of conflicts in routing. Furthermore, the energy usage and vehicle charging are integrated in the model.

The main contributions of this paper are:

1) We propose a strategic and a disrupted MILP model for vehicle-to-aircraft assignment which facilitates disruption management throughout a day of operations.
2) We include an energy usage and charging model, conflict and collision avoidance, and realistic model parameters.
3) We apply our models to a case study at a large hub airport and investigate the effect of varying model parameters and inputs.

The remainder of this paper is organized as follows: in Section II the framework of and inputs to the strategic model for vehicle-to-aircraft assignment are introduced, including the aircraft and vehicle path planning and the ETV energy model. Then, the MILP formulation is stated and explained. In Section III the disrupted MILP model is formulated and its usage is illustrated. In Section IV the models introduced in Section II and III are applied to Amsterdam Airport Schiphol to obtain series of vehicle-to-aircraft assignments. In Section V sensitivity analysis is performed on the models by varying model parameters and inputs. Finally, Section VI summarizes the findings and recommendations for future work.

II. Strategic Management of Electric Taxiing Vehicles Towing Aircraft

In this section we propose a model that generates an assignment of departing and arriving aircraft to a fleet of ETVs. These ETVs electrically tow the aircraft assigned to them, and are charged at charging stations when required.

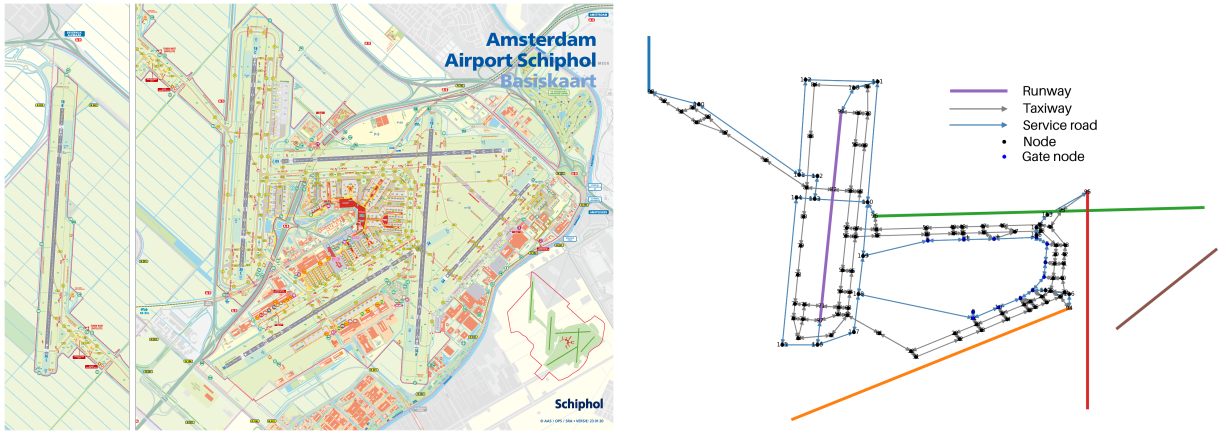

(a) Technical map, displaying all roads, runways, gates and buildings [21].

(b) Graph representation of the airport, $G_X \cup G_S$, including the runways, gates, taxiways and service roads.

Fig. 1 Maps of Amsterdam Airport Schiphol.

A. Airport layout

An airport is represented by two graphs, with some shared nodes and edges: the taxiway graph $G_X = (N_X, E_X)$ and the service road graph $G_S = (N_S, E_S)$. All edges in E_S are two-directional, and some edges in E_X are one-directional.

In this paper Amsterdam Airport Schiphol (EHAM) will be used as the reference airport. Figure 1a shows a technical map of this airport, and Figure 1b shows the graph representation used for the models presented in this paper. It highlights the taxiways and service roads used to reach the five considered runways. The many gates of the airport are grouped into several gate nodes. The runways are assumed to use only one exit/entry point, and at this point the runway node is located. Furthermore, nodes n_5, n_{108} and n_{110} are designated as charging stations. Formally, the set of charging stations $S_{\text{cs}} = \{n_{\text{cs},i} : i \in \{1, ..., N_{\text{cs}}\}\} = \{n_5, n_{108}, n_{110}\}$ and its total number is $N_{\text{cs}} = 3$. Lastly, node n_5 also functions as the ETV depot n_{dp}.

Taxiing aircraft and ETVs towing aircraft are allowed to drive on the taxiways, where a maximum speed of v_x holds. ETVs that are not towing aircraft are allowed to drive on the service roads, where a maximum speed of v_s holds. Although not all airports have a network of service roads available, it is assumed in this work that airports that implement a fleet of ETVs will also implement a service road network. This is because it would be very difficult to route both the aircraft and the travelling ETVs along the taxiways, while retaining the same throughput of flights [22, 23].

We define the distance metrics $d_X(m, n)$ and $d_S(m, n)$ for G_X and G_S, respectively. These distances are the shortest distances within the graphs, which are calculated using Dijkstra's algorithm.

B. Aircraft path planning

Before we perform vehicle-to-aircraft assignment, we create the routes the aircraft have to traverse. The assignment is made for a certain time period $T = [t^s, t^e]$ on a certain day. The aircraft a that arrive or depart at the reference airport within T form the set A. The number of aircraft within A is denoted as N^F.

Given the flight schedule for that day, we collect the scheduled times of arrival or departure of all aircraft within T. More specifically, the scheduled landing time (SLDT) of an arriving flight or the scheduled off-block time (SOBT) of a departing flight is used, since that is the moment a towing vehicle can start to interact with the aircraft. We will refer to this time as the pick-up time of aircraft a: t_a^p. The time an ETV has finished towing the aircraft is referred to as the drop-off time t_a^d. Furthermore, the pick-up and drop-off locations n_a^p and n_a^d are obtained from the flight schedule and airport layout. For a departing aircraft, the pick-up node is a gate node and the drop-off node is a runway node, and for an arriving aircraft, vice versa.

Using the distance metric d_X defined in Section II.A, we calculate the time needed to traverse the distance between any pair of nodes on G_X as:

$$t_X(m, n) = d_X(m, n)/v_x \quad \forall m, n \in G_X. \tag{1}$$

This means that the drop-off time of aircraft a is calculated as:

$$t_a^d = t_a^p + t_X(n_a^p, n_a^d) \quad \forall a \in A. \tag{2}$$

It is assumed that no delay is incurred during taxiing due to reasons such as malfunctioning vehicles or aircraft or weather events. However, it is possible that aircraft incur delay because they have to make use of the same nodes or edges at the same time as another aircraft. Furthermore, the minimum separation distance d_{sep} between two aircraft should be respected and is set at 200 m [17, 24]. Since the taxiway speed v_x is roughly 10 m/s, the separation time t_{sep} is set at 20 s.

It is necessary to select which aircraft has to wait at which moment in order to resolve potential conflicts or separation violations. This we refer to as *deconflicting routes*. Using the routes, including the time at which each node is reached, the pick-up and drop-off nodes and times for each aircraft, the schedule is deconflicted before performing the vehicle to flight assignment. The route for each aircraft is defined as a series of nodes $n^{\text{route}} = \{n_p^a, ..., n_d^a\}$ and the times the aircraft is to arrive at those nodes as a series of times $t^{\text{route}} = \{t_p^a, ..., t_d^a\}$.

Algorithm 1 summarizes the deconflicting procedure. The procedure runs through a series of time steps, separated from the previous by time step $\Delta = t_{\text{sep}}$, and through all aircraft $a \in A$. If aircraft a will reach a node within this time step, the algorithm checks for two situations. First, it checks whether another aircraft $b \in A$ will reach the same node within the same time step. If there is such an aircraft, the rest of the route of aircraft a is postponed by one time step Δ. Second, when a is about to enter a two-directional edge $x \in E_X$, the algorithm looks for an aircraft b on the set of edges E_x^{bi} that have to be free from oncoming traffic before a can enter x. For example, let $x = (n_{81}, n_{86})$, see Fig 1b. Then $E_x^{\text{bi}} = \{(n_{86}, n_{81}), (n_{87}, n_{86})\}$. If an aircraft b is on either of these edges at the current time step, the rest of the route of aircraft a is postponed by the amount of time needed for b to clear these edges.

Algorithm 1 Deconflict routes

Require: $t_a^{\text{route}}, n_a^{\text{route}}$ $\forall a \in A$, $\quad E_x^{\text{bi}}$ $\forall$edges x in the set of two-directional edges in E_X
- **for** $i = 0, 1, 2, ...$ **do**
  - $t \leftarrow t^s + i\Delta$
  - **for** $a = 0, 1, 2, ..., N^F$ **do**
    - **if** $\exists j : a$ reaches $n_{a,j}^{\text{route}}$ within Δ **then**
      - **if** $\exists$ aircraft b that reaches $n_{a,j}^{\text{route}}$ within Δ **then**
        - **for** $k = j, ..., |n_a^{\text{route}}|$ **do**
          - $t_{a,k}^{\text{route}} = t_{a,k}^{\text{route}} + \Delta$
          - $t_a^d = t_a^d + \Delta$
        - **end for**
      - **else if** $(n_{a,j}^{\text{route}}, n_{a,j+1}^{\text{route}})$ is a two-directional edge **then**
        - $x \leftarrow (n_{a,j}^{\text{route}}, n_{a,j+1}^{\text{route}})$
        - **for** $i_x \in E_x^{\text{bi}}$ **do**
          - **if** $\exists$ aircraft b that will be on i_x within Δ **then**
            - **for** $k = j, ..., |n_a^{\text{route}}|$ **do**
              - $t_{a,k}^{\text{route}} = t_{a,k}^{\text{route}} + \Delta \frac{t_X(i_x)}{v_x}$
              - $t_a^d = t_a^d + \Delta \frac{t_X(i_x)}{v_x}$
            - **end for**
          - **end if**
        - **end for**
      - **else**
        - Register that aircraft a reaches node $n_{a,j}^{\text{route}}$ within Δ
      - **end if**
    - **end if**
  - **end for**
- **end for**

Figure 2 shows the averaged and total minutes of delay incurred due to the deconflicting procedure, during any ten minute interval during two different periods T. Figure 2a shows that very few adjustments are necessary on the

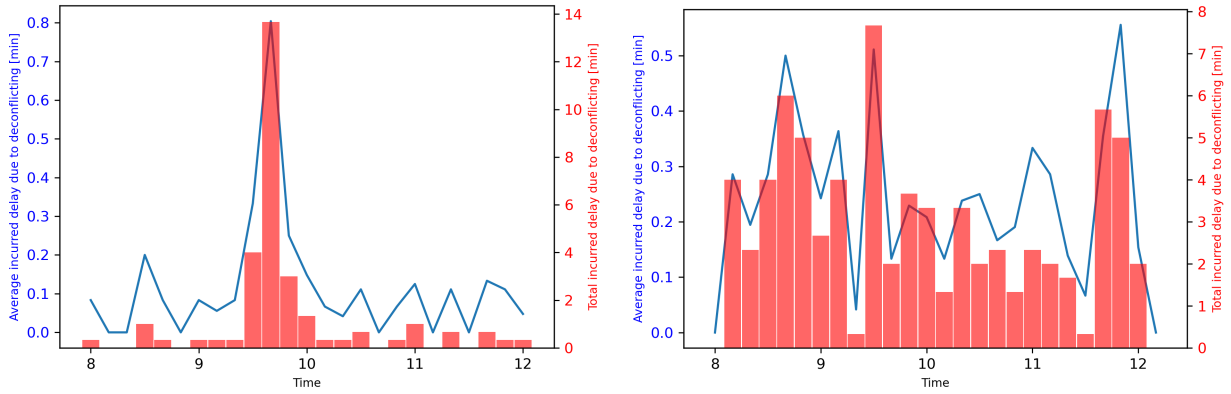

(a) The delay incurred due to the deconflicting procedure on March 27th 2022 from 08:00 to 12:00 (148 aircraft).

(b) The delay incurred due to the deconflicting procedure on December 27th 2021 from 08:00 to 12:00 (286 aircraft).

Fig. 2 The delay incurred to the deconflicting aircraft during a quiet period and during a busy period.

morning of March 27th 2022, which is a quiet day, save for the arrival peak from 09:30-10:00. Figure 2b shows that on the morning of December 27th 2021, a busy day, many more adjustments are necessary. However, in none of the intervals the average incurred delay exceeds one minute. In addition, one could argue that for actual operation, these delays will be even smaller. This is because part of the delays now attributed to deconflicting during the taxiing period, will in fact be incurred during holding in the air (for arrivals) or waiting at the gate (for departures). This is because the model uses the scheduled off-block and landing times, rather than the actual times.

C. Vehicle path planning

With the aircraft path planning defined, we now turn to ETV path planning. The ETV fleet V with size N^V is assumed to leave the depot n_{dp} at the start of time period T. Each ETV v travels to the pick-up point n_a^p of its assigned aircraft a via the service road network G_S. It arrives at the aircraft at time $t_a^p - t^c$, where it starts the connecting procedure, which takes t^c. At t_a^p the ETV starts towing the aircraft via the taxiway network G_X to its destination, n_a^d. After arriving there at time t_a^d, the disconnecting procedure takes place, lasting until $t_a^d + t^c$. The ETV will then either wait at its location for some time, start to travel to another assigned aircraft, or start to travel to one of the charging stations $n_{\text{cs},i}$.

As in Section II.B, we use the distance metric d_S defined in Section II.A to calculate the time needed to traverse the distance between any pair of nodes on G_S as:

$$t_S(m,n) = d_S(m,n)/v_s \quad \forall m,n \in G_S. \tag{3}$$

The ETVs travel on the service road network G_S when they do not tow aircraft. The service roads are assumed to provide enough opportunities to pass oncoming traffic. Furthermore, no significant separation distance is required between the ETVs. For these reasons, the vehicle path planning is limited to calculating the shortest paths and associated times between destinations of the ETVs, but no deconflicting procedure is required.

The needed jet engine warm-up procedure is assumed to take place during the towing, and the cool-down procedure takes place when the ETV is disconnected after taxi-in. This means that both procedures have no influence on the ETV path planning.

D. ETV energy consumption and charging

In order to keep track of the state of charge (SOC) of the individual ETVs, it is necessary to determine how fast the ETV batteries charge at a charging station, and discharge while driving or towing an aircraft. For the latter, we are interested in calculating the power $P(v, m_a)$ consumed by an ETV towing a mass m_a at speed v. This can be approximated by considering the rolling resistance and the thrust as the only forces acting on the ETV or ETV + aircraft combination, disregarding e.g. drag or slope of the airport roads. The power consumed is then equal to the rolling force

times the velocity, where the rolling force is equal to the rolling resistance coefficient times the normal force, i.e. gravity. Thus we obtain:

$$P(v, m) = \mu^g(v) g (m_{\text{ETV}} + m_a) v, \tag{4}$$

with

$$\mu^g(v) = \mu^0 (1 + \frac{v}{v^0}) \tag{5}$$

the rolling resistance coefficient at speed v, m_{ETV} the mass of the ETV, m_a the mass of aircraft a, g the gravitational acceleration, μ^0 the rolling resistance base coefficient and v^0 the rolling resistance base velocity [25].

Using Eq. 4 we calculate the power consumed by ETV during towing aircraft a, $P(v_x, m_a)$, and during driving, $P(v_s, 0)$. The charging power, denoted as P^c, is dependent on the capabilities of the ETV battery and the charging infrastructure at the airport.

In this work a constant speed is assumed to be attained by the ETV at all times, without accounting for acceleration and deceleration. With this information and the expressions for power defined above, we can introduce notation for the energy q required to perform certain movements:

$$q^X(a) = P(v_x, m_a) t_X(n_a^p, n_a^d) \qquad \forall a \in A, \tag{6}$$

$$q^S(n, m) = P(v_s, 0) t_X(n, m) \qquad \forall m, n \in N_S, \tag{7}$$

$$q^S(a, b) = q^S(n_a^d, n_b^p) \qquad \forall a, b \in A, \tag{8}$$

$$q_f^S(v, a) = q^S(n_v^{\text{old}}, n_a^p) \qquad \forall a \in A, v \in V, \tag{9}$$

$$q_l^S(a) = q^S(n_a^d, n_{\text{dp}}) \qquad \forall a \in A, \tag{10}$$

$$q^C(a, b) = \min_{i \leq N_{\text{cs}}} \{q^S(n_a^d, n_{\text{cs},i}) + q^S(n_{\text{cs},i}, n_b^p)\} \qquad \forall a, b \in A, \tag{11}$$

$$q_s^C(a) = \min_{i \leq N_{\text{cs}}} \{q^S(n_{\text{cs},i}, n_a^p)\} \qquad \forall a \in A. \tag{12}$$

Here $q^X(a)$ is the energy required by an ETV to tow aircraft a along the taxiways, $q^S(n, m)$ is the energy required by an ETV to travel from node n to m along the service roads, $q^S(a, b)$ is the energy required by an ETV to travel from the dropoff point of aircraft a to the pickup point of aircraft b along the service roads, $q_f^S(v, a)$ is the energy required by ETV v to travel from its latest location, n_v^{old}, to the pickup point of aircraft a, $q_l^S(a)$ is the energy required by an ETV to travel from the dropoff point of aircraft a to the depot, $q^C(a, b)$ is the energy required by an ETV to travel from the dropoff point of aircraft a to the pickup point of aircraft b along the service roads and via the closest charging station, and $q_s^C(a)$ is the energy required by an ETV to travel from the closest charging station to the pickup point of aircraft a. Last, we denote the maximum energy capacity of an ETV by Q.

E. MILP formulation for vehicle-to-aircraft assignment

After the deconflicting procedure, the updated values of t_a^p and t_a^d are used to generate sets of aircraft used in creating the constraints of the MILP model. Before introducing the MILP formulation, we define:

$$t^C(a, b) = t_b^p - t_a^d - t_S(n_a^d, n_b^p) - 2t^c \qquad \forall a, b \in A, \tag{13}$$

which is the available time between towing aircraft a and b that can be used for idling or travelling to charging stations and charging. Then:

$$A_{\text{out}}(a) = \{b \in A : t^C(a, b) > 0\} \qquad \forall a \in A, \tag{14}$$

$$A_{\text{in}}(a) = \{b \in A : t^C(b, a) > 0\} \qquad \forall a \in A, \tag{15}$$

$$A_{\text{PC}}(a) = \{b \in A_{\text{out}}(a) : q^C(a, b) - q^S(a, b) < P^c(t^C(a, b) - t_{\text{min}}^C)\} \qquad \forall a \in A, \tag{16}$$

where $A_{\text{out}}(a)$ is the set of aircraft that can be towed by an ETV after it tows aircraft a, $A_{\text{in}}(a)$ is the set of aircraft that can be towed by an ETV before it tows aircraft a, and $A_{\text{PC}}(a)$ is the set of aircraft that can be towed by an ETV after it tows aircraft a and for which there is at least t_{min}^C time in between for effective charging. Effective charging is the

charging that occurs after the energy loss due to the rerouting to the charging station has been replenished. Note that $A_{\text{PC}}(a) \subseteq A_{\text{out}}(a)$.

The MILP formulation in this work is based on that of van Oosterom et al. [16]. We consider the following decision variables:

$$x_{ab} = \begin{cases} 1 & \text{if } a, b \in A \text{ are towed consecutively} \\ 0 & \text{else} \end{cases} \tag{17}$$

$$x^f_{av} = \begin{cases} 1 & \text{if } a \in A \text{ is the first aircraft towed by ETV } v \in V \\ 0 & \text{else} \end{cases} \tag{18}$$

$$x^l_a = \begin{cases} 1 & \text{if } a \in A \text{ is the last an ETV tows} \\ 0 & \text{else} \end{cases} \tag{19}$$

$$q_a \in [q^X(a), Q] \quad \text{ETV state of charge at the start of towing } a \in A \tag{20}$$

$$y_a = \begin{cases} 1 & \text{if } a \in A \text{ is towed by an ETV} \\ 0 & \text{if } a \in A \text{ is taxiing by itself} \end{cases} \tag{21}$$

The objective function and constraints are given by:

$$\max_{x,q,y} \quad (1-\alpha) \sum_{a \in A} y_a, \tag{22}$$

$$\text{s.t.} \quad \sum_{v \in V} x^f_{av} + \sum_{b \in A^{\text{in}}_a} x_{ba} = y_a \qquad \forall a \in A, \tag{23}$$

$$\sum_{b \notin A^{\text{in}}_a} x_{ba} = 0 \qquad \forall a \in A, \tag{24}$$

$$x^l_a + \sum_{b \in A^{\text{out}}_a} x_{ab} = y_a \qquad \forall a \in A, \tag{25}$$

$$\sum_{b \notin A^{\text{out}}_a} x_{ab} = 0 \qquad \forall a \in A, \tag{26}$$

$$q_a \le Q(1 - x^f_{av}) + x^f_{av}(q^{\text{first}}_v - q^S_f(v,a)) \qquad \forall a \in A, v \in V, \tag{27}$$

$$q_a \ge -Q(1 - x^f_{av}) + x^f_{av}(q^{\text{first}}_v - q^S_f(v,a)) \qquad \forall a \in A, v \in V, \tag{28}$$

$$0 \le q_a - x^l_a(q^X(a) + q^S_l(a)) \qquad \forall a \in A, \tag{29}$$

$$q_b \le q_a - x_{ab}(q^X(a) + q^S(a,b)) + Q(1 - x_{ab}) \qquad \forall a \in A, b \in A^{\text{out}}_a \setminus A^{\text{PC}}_a, \tag{30}$$

$$q_b \le Q - x_{ab} q^C_s(b) \qquad \forall a \in A, b \in A^{\text{PC}}_a, \tag{31}$$

$$q_b \le q_a - x_{ab}(q^X(a) + q^C(a,b) - P^c t^C(a,b)) + Q(1 - x_{ab}) \qquad \forall a \in A, b \in A^{\text{PC}}_a, \tag{32}$$

$$q_b \ge q_a - x_{ab}(q^X(a) + q^S(a,b)) - Q(1 - x_{ab}) \qquad \forall a \in A, b \in A^{\text{out}}_a, \tag{33}$$

$$N^V \ge \sum_{a \in A} x^l_a, \tag{34}$$

$$\sum_{a \in A} x^f_{av} = 1, \qquad \forall v \in V, \tag{35}$$

$$\sum_{v \in V} x^f_{av} \le 1, \qquad \forall a \in A, \tag{36}$$

The objective (22) is to maximize the number of aircraft towed by the fleet of ETVs. The factor $(1-\alpha)$ preceding the expression is there to ensure consistency with the disrupted model, which will be described in the next section. Constraints (23) and (25) ensure that every aircraft a that is towed by an ETV, is either the first (last) to be towed by an ETV, or has another aircraft b preceding (following) it. Constraints (24) and (26) ensure that an aircraft b that is not in A^{in}_a (A^{out}_a) cannot precede (follow) aircraft a. Constraints (27), (28) and (29) make sure that ETVs start with a full

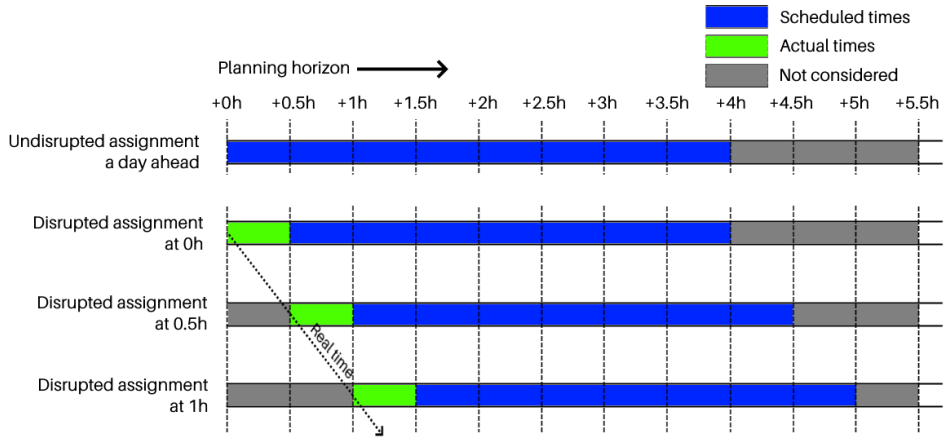

Fig. 3 Usage of the strategic and disrupted model when creating vehicle-to-aircraft assignments during a day of operations, with an indication of when scheduled or actual arrival and departure times are considered.

battery at their first task, and have enough energy at the end of the period T to reach the depot. ETV v starts with a state of charge of q_v^{first} at t^s. In the strategic model the ETVs are assumed to start with a full battery ($q_v^{\text{first}} = Q$). Later, in the disrupted model, the state of charge of ETV v in any assignment will be taken from the previously generated assignment.

Constraint (30) subtracts the energy spent on towing aircraft a from the state of charge of aircraft b, if no charging has taken place in between. Constraint (31) limits the state of charge to Q after a period of charging. Constraint (32) adds the energy gained from charging to the SOC of an ETV. Constraint (33) limits the reduction in SOC to only what was spent on towing aircraft a. Constraint (34) limits the number of used ETVs to the maximum of N^V. Constraint (35) ensures that for every ETV v, only one aircraft is the first to be towed by that ETV. Constraint (36) ensures that for every aircraft a, no more than one ETV is assigned to be the first to tow it.

The advantage of MILP formulation (22)-(36) is that it is possible to determine all times and durations of all activities of the ETVs and aircraft from the given decision variables, without having to introduce a variable x_{abv}. This would create $N^F \cdot N^F \cdot N^V$ variables, whereas now the number of variables remains of the order $N^F \cdot N^F$. The usage of x_{av}^f rather than x_a^f (parallel to x_a^l) ensures that the model assigns a task list of aircraft to a specific vehicle, rather than obtaining N^V task lists that are not tied to any specific vehicle. This will be essential in the disrupted model, which is introduced in the next section.

III. Disruption Management of Electric Taxiing Vehicles Towing Aircraft

The disrupted model is used to obtain a vehicle-to-aircraft assignment based on a flight schedule that partly consists of actual departure and arrival times, rather than scheduled times. When creating assignment for a given day of operations, both models are used. Figure 3 shows in what order the models are used. An initial assignment of the first four hours of operation is made in advance of t^s, using the strategic model. After this, the disrupted model is run every half hour for the four hours of operation directly after that moment, so that t^s is right after the moment of running the model. It is assumed that the flight delays of aircraft departing and arriving in the coming half hour are known at the moment of using the model. That means that for this period, the actual times of arrival and departure are used to compute the assignment, rather than the scheduled times. At the first instance of running the disrupted model, the previously obtained assignment is the result of the strategic model. At the second and later instances, the previous assignment has come from the disrupted model.

The goal of the disrupted model is to obtain an assignment that is close to the previously obtained assignment, i.e. we would like to minimize the number of changes to the towing schedule for ETV operators. In order to quantify this, we introduce an additional decision variable for the disrupted model:

$$s_v = \begin{cases} 1 & \text{if for vehicle } v \in V \text{ the list of aircraft to tow has remained the same as in the previous assignment} \\ 0 & \text{else.} \end{cases} \tag{37}$$

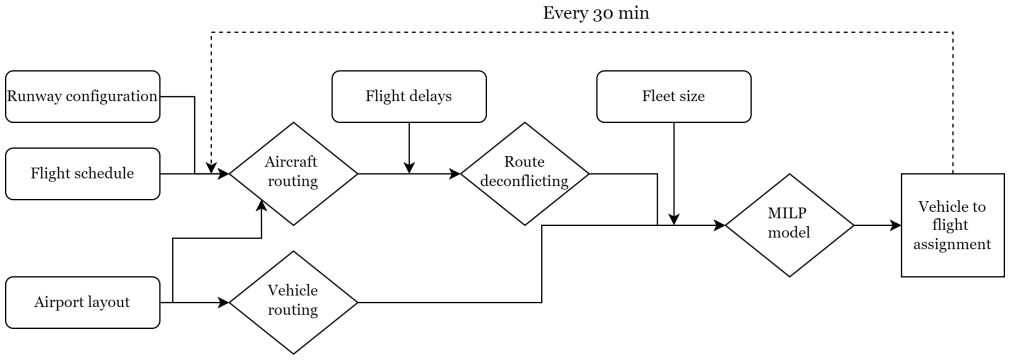

Fig. 4 Flowchart for the usage of the disrupted model, containing inputs, outputs and processes. Every 30 minutes, the model is applied.

When creating an assignment for the next time period T, the aircraft that are towed by vehicle v in the first half hour of the previous time period will have disappeared from the schedule. Likewise, new aircraft will be added to the schedule for the last half hour of this new period. The "list of towed aircraft" in Eq. 37 refers to all but these aircraft. The variable has the value 1 if the aircraft are still to be towed by vehicle v in the new assignment, and in the same order as before.

The objective function (22) of the strategic model is replaced by Eq. (38):

$$\max_{x,q,y,s} \quad (1-\alpha)\sum_{a\in A} y_a + \alpha \sum_{v\in V} s_v. \tag{38}$$

The objective function (38) now contains two terms; the number of aircraft towed, and the number of vehicles with an unchanged schedule. By varying the parameter α, the trade-off between these terms can be controlled. Since both terms will be used many times throughout this paper, we introduce shorthand notation, reducing objective function (38) to:

$$\max_{x,q,y,s} \quad (1-\alpha)Y + \alpha S. \tag{39}$$

Constraints (23)-(36) are the same as in the strategic model. Some additional constraints are added:

$$M(1-s_v) \geq N_v^F + 1 - \sum_{i=1}^{N_v^F} x_{f_{vi}t_{vi}} - x^f_{f_{v0}v} \qquad \forall v \in V, \tag{40}$$

$$1 - s_v \leq N_v^F + 1 - \sum_{i=1}^{N_v^F} x_{f_{vi}t_{vi}} - x^f_{f_{v0}v} \qquad \forall v \in V, \tag{41}$$

$$x^f_{av} = 1, \qquad \forall a \in A, v \in V : x^{f,\text{old}}_{av} = 1 \tag{42}$$

where $N_v^F + 1$ is the number of aircraft that are towed sequentially in the previous solution for ETV $v \in V$ and also appear in the current period T, f_{vi} is the i-th aircraft from which ETV v departed in the previous solution, t_{vi} is the i-th aircraft at which ETV v arrived in the previous solution, M is a large value, and $x^{f,\text{old}}_{av}$ is the value of x^f_{av} from the previous assignment.

Constraints (40) and (41) define s_v. Constraint (42) guarantees continuity between the current and previous assignment, by assigning the aircraft that were being towed when the new assignment was made to the correct ETVs. The path planning, deconflicting procedure and energy model remain the same as for the strategic model.

Figure 4 shows a flowchart for the usage of the disrupted model introduced in this section. It shows where the inputs are used, e.g. the flight delays are first applied to the aircraft routes, before the routes are deconflicted. After obtaining the solution, it is used in the next time period to obtain the new aircraft routes.

IV. Results

In this section the strategic and disrupted model are applied to create vehicle-to-aircraft assignments for aircraft arriving and departing at the reference airport Amsterdam Airport Schiphol. Flight schedules are taken from historical

data, provided by the Schiphol Developer Center [26]. From these flight schedules the gate numbers and the scheduled and actual off-block time or landing time are obtained. The runway configuration of any day in the past is available from Dutch Air Traffic Control [27, 28].

The choices of parameter values are summarized in Table 1.

Table 1 Parameter values for the assignment models.

Symbol	Name	Value	Unit	Source
d_{sep}	Separation distance	200	m	[17]
v_s	Speed on service roads	30	km/h	[29, 30]
v_x	Speed on taxiways	42	km/h	[31]
t^c	Connecting/Disconnecting time	3.0	min	[32]
t^C_{min}	Minimum charging time	30	min	
μ^0	Rolling resistance base coefficient	0.010	-	[25]
v_0	Rolling resistance base velocity	41.2	km/h	[25]
m_a	Aircraft mass	$8.0 \cdot 10^4$	kg	
m_{ETV}	ETV mass	$1.45 \cdot 10^4$	kg	[13]
P^c	Charging power	100	kW	[16]
Q	Battery capacity	400	kWh	[16]

The model assumes one weight class of aircraft, with a mass of $8.0 \cdot 10^4$ kg (the maximum take-off weight of a Boeing 737-800), and one type of ETV. The model can be extended to include several weight classes in both the aircraft and the ETVs, see for example van Oosterom et al. [16]. The mass of the ETV is calculated as

$$m_{\text{ETV}} = m_0 + m_q Q, \tag{43}$$

where m_0 is the base mass and m_q is the battery energy density. Given a base mass of $1.2 \cdot 10^4$ kg [13] and an energy density of 6.25 kg/kWh [16], we arrive at the value given in Table 1.

Current fast-charging technology might allow for a greater charging power than $P^c = 100$ kW. However, the energy load on the airport's network will have to remain bearable even when several ETVs are charging at the same time [33]. The minimum charging time is chosen such that the model will not generate a schedule where ETVs travel to charging stations to only charge for a few minutes. An ETV will charge either for at least t^C_{min} or until the state of charge reaches Q.

A. Example day of operations

Figures 5 and 6 show the vehicle-to-aircraft assignments obtained using the strategic and disrupted model for December 27th 2021. First, in Fig 5a, the strategic model is run to obtain an initial assignment for the period 08:00-12:00, based on the scheduled off-block and landing times. Then, in Fig 5b the disrupted model is run for the same period, but now using the actual times for the first half hour. In Fig 6a and Fig 6b the period is shifted by half an hour and the disrupted model is applied again. The calculations were performed using Gurobi 9.5 on a Dell Latitude 7490 laptop with an Intel i7-8650U CPU of 1.90 GHz.

In this example, α is set to 0.999, i.e. the second term of objective function (38) from the disrupted model is made the most important; S is prioritized over Y. Furthermore, N^V is set to 40, which is mostly enough to tow all aircraft that arrive and depart during the time period T.

Using black and blue coloring, Figs 5 and 6 show for individual aircraft whether they are still following the same aircraft as in the previous assignment, i.e. if for aircraft b the value of $x_{ab} = 1$ in the previous assignment, then this is still the case in the current assignment. When a towing schedule has changed for an ETV, we can see that this is due to delays of the aircraft in this schedule. Take for example ETV 24 in Fig 5b: aircraft 1666 follows aircraft 1368. However, in Fig 6a we see that this cannot be maintained: aircraft 1666, which had a scheduled landing time of 08:45, arrives 11 minutes early. ETV 24 would not have enough time to travel between these tasks, i.e. from n^d_{1368} to n^p_{1666}. In the new schedule aircraft 1666 is towed by ETV 7.

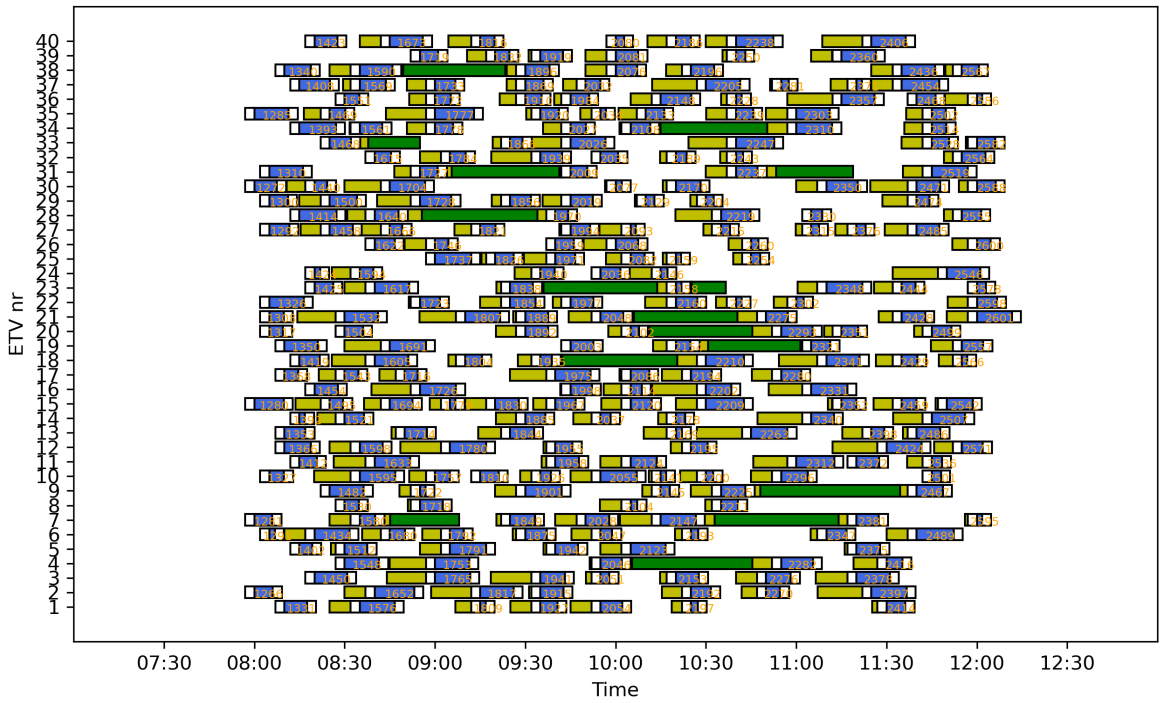

(a) The vehicle-to-aircraft assignment obtained using the strategic model for 08:00-12:00.

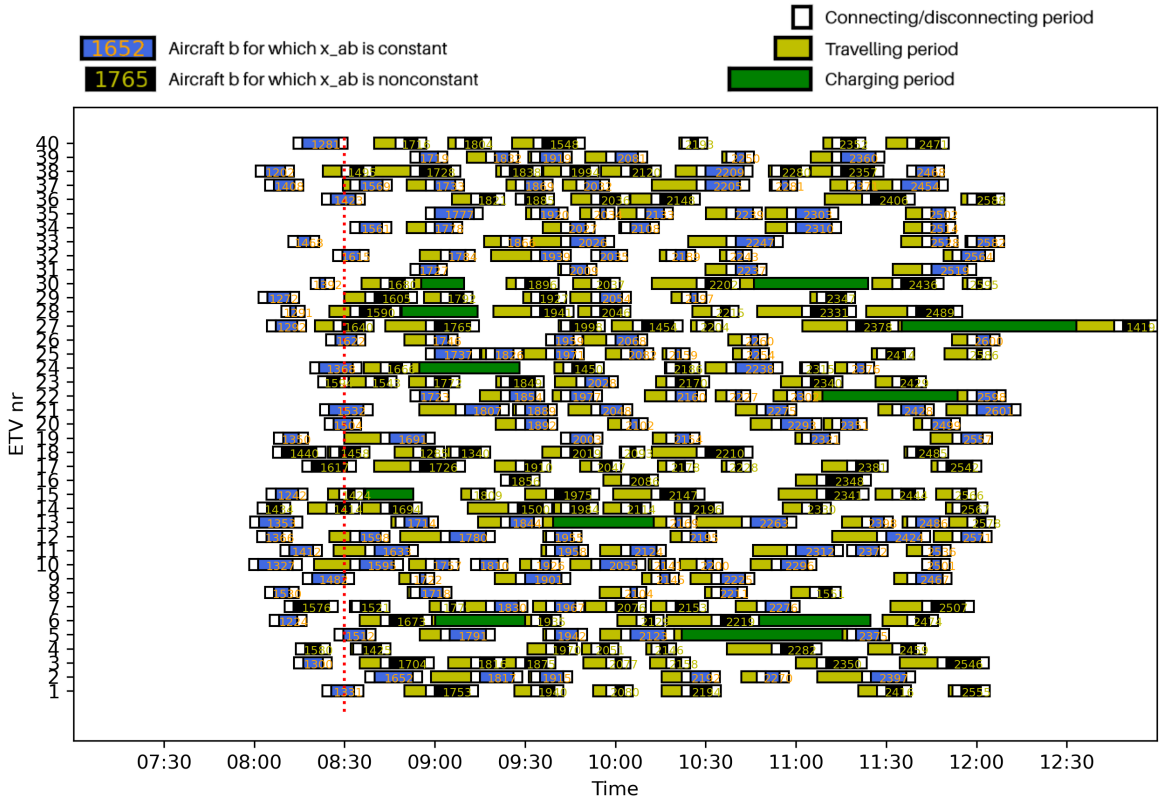

(b) The vehicle-to-aircraft assignment obtained using the disrupted model for 08:00-12:00.

Fig. 5 Vehicle-to-aircraft assignments for December 27th 2021. A red dashed line indicates the time until which the disruptions are considered known.

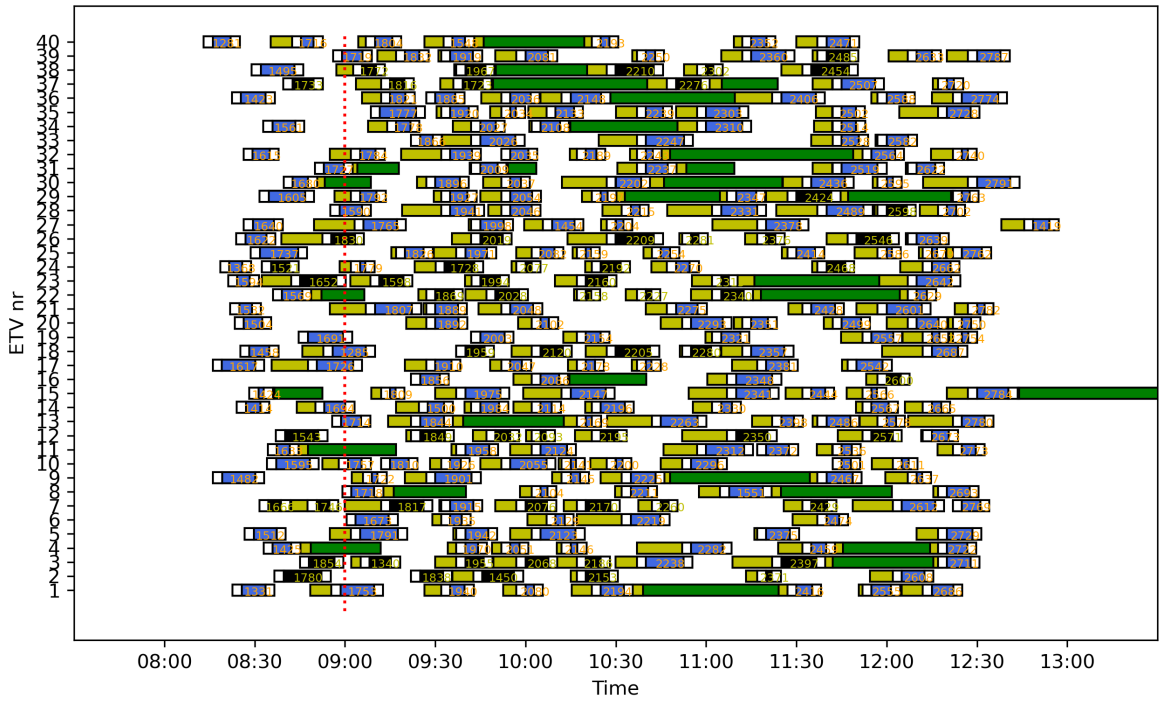

(a) The vehicle-to-aircraft assignment obtained using the disrupted model for 08:30-12:30.

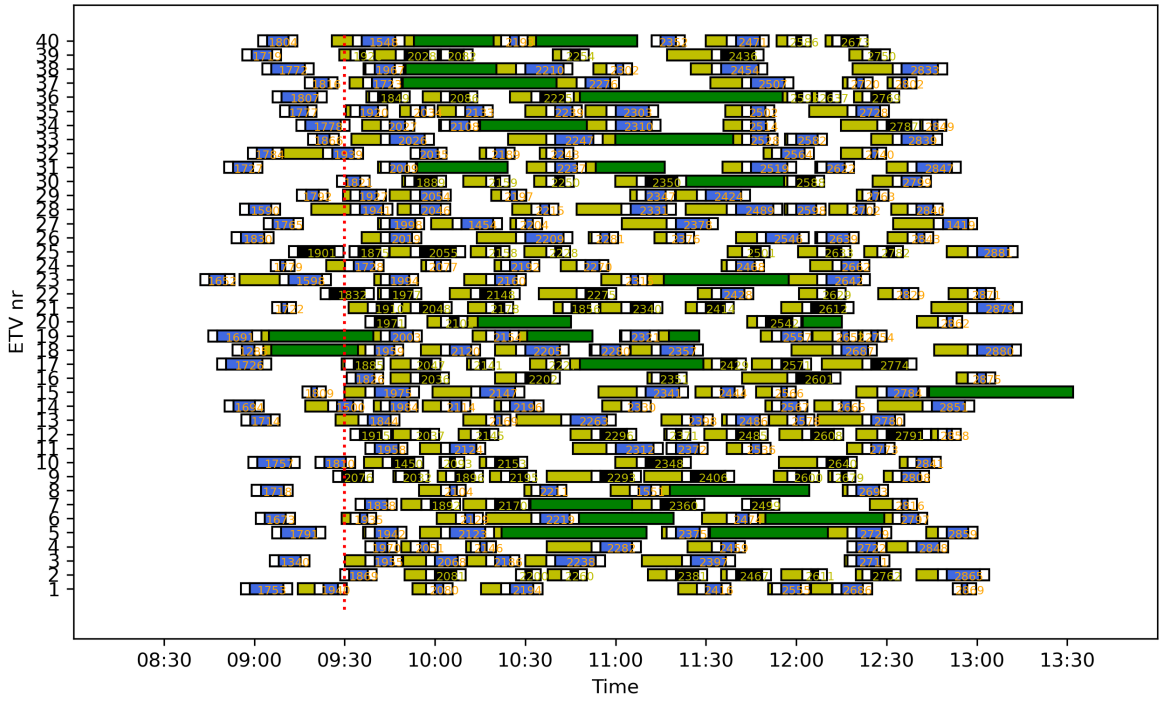

(b) The vehicle-to-aircraft assignment obtained using the disrupted model for 09:00-13:00.

Fig. 6 Continuation of Figure 5.

Table 2 Objective values for vehicle-to-aircraft assignments of December 27th 2021 with $N^V = 40$.

Model	t^s	t^e	Objective	Y	N^F	S	Solution time
Strategic	08:00	12:00	00.286	286	286	N/A	39.5
Disrupted	08:00	12:00	21.259	280	280	21	18.6
Disrupted	08:30	12:30	29.266	295	297	29	15.5
Disrupted	09:00	13:00	26.261	287	289	26	13.6
Disrupted	09:30	13:30	15.269	294	284	15	21.3
Disrupted	10:00	14:00	09.266	275	275	09	14.6
Disrupted	10:30	14:30	22.253	275	275	22	16.1
Disrupted	11:00	15:00	24.231	255	258	24	11.7
Disrupted	11:30	15:30	18.234	252	255	18	12.7
Disrupted	12:00	16:00	22.229	251	251	22	10.8
Disrupted	12:30	16:30	18.225	243	244	18	11.8
Disrupted	13:00	17:00	21.225	246	246	21	12.5
Disrupted	13:30	17:30	22.212	234	236	22	09.8
Disrupted	14:00	18:00	21.205	226	226	21	13.5
Disrupted	14:30	18:30	30.181	211	211	30	06.9
Disrupted	15:00	19:00	32.175	207	207	32	06.6

From these figures we can deduct that the disrupted model is able to keep the list of aircraft to tow the same for a significant amount of the ETVs. Table 2 shows the results of applying the disrupted model throughout the day. The number of unchanged schedules, i.e. $S = \sum_{v \in V} s_v$, displayed in the penultimate column, appears to be roughly inversely correlated with the total number of aircraft in the time period. This corresponds with intuition: if the number of aircraft is smaller, but the number of ETVs remains the same, every ETV has fewer aircraft to tow, and its schedule is less prone to the disruptions of flight delay. Second, by averaging the values for S we obtain that on December 27th 2021, roughly 22 out of 40 vehicles, i.e. 55%, receive an unchanged schedule in every time period.

Figure 7 shows the state of charge of every ETV during two of the periods appearing in Table 2. In Fig. 7a we see that all ETVs start with a state of charge near the maximum, Q, and are sometimes recharged to full capacity within the time period T. In Fig. 7b we see that some ETVs are being recharged by a considerable amount, but many of them have run out of charge. This means that under this model, charging during the day will need to be supplemented with night charging.

B. Trade off between objective terms

The objective function (38) consists of two terms. It maximizes both the number of aircraft towed, Y, and the number of ETVs for which the assignment is unchanged, S. In this section we investigate the effect of prioritizing one term over the other.

We consider a situation where not all aircraft can be towed by the fleet of ETV: let $N^V = 25$. Then we run the disrupted model, while varying α. The results are shown in Table 3, where values for both terms of the objective function (38) are displayed for several values of α. We see that when decreasing α, the number of unchanged schedules S decreases, and the number of towed aircraft Y increases slightly. When $\alpha = 0.3$, an extra aircraft towed contributes the same to the objective as two more ETVs with unchanged schedules. When $\alpha = 0.999$, the unchanged schedules contribute a thousand times more to the objective than the towed aircraft. When $\alpha = 0.001$ we obtain the opposite. From Table 3 it can be concluded that for December 27th 2021 and with the current model parameters, the results do not vary greatly with varying α values. In order to obtain the maximum number of unchanged schedules S, a maximum of five aircraft (2%) will have to taxi by themselves. This means that it is possible to pursue practicality for ETV operators (number of unchanged schedules), while retaining the minimization of environmental impact (number of towed aircraft).

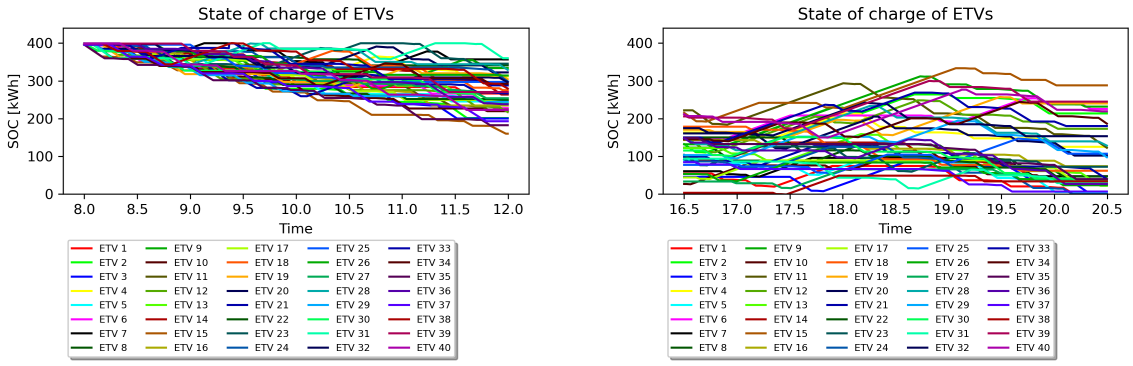

(a) State of charge graphs during 08:00-12:00, obtained with the disrupted model.

(b) State of charge graphs during 16:30-20:30, obtained with the disrupted model.

Fig. 7 State of charge of all ETVs during two different time periods on December 27th 2021 at Schiphol Airport.

Table 3 Objective values for vehicle-to-aircraft assignments with varying α of December 27th 2021 with $N^V = 25$.

			$\alpha = 0.001$		$\alpha = 0.3$		$\alpha = 0.7$		$\alpha = 0.999$	
Model	t^s	t^e	Y	S	Y	S	Y	S	Y	S
Strategic	08:00	12:00	266	N/A	266	N/A	266	N/A	266	N/A
Disrupted	08:00	12:00	263	6	263	3	262	8	260	8
Disrupted	08:30	12:30	280	6	280	4	276	10	275	9
Disrupted	09:00	13:00	272	7	271	7	269	8	271	8
Disrupted	09:30	13:30	272	3	272	2	271	1	271	4
Disrupted	10:00	14:00	269	0	269	0	268	1	268	1

Table 4 Number of unchanged schedules, S, for vehicle-to-aircraft assignments obtained with the disrupted model, when varying N^V, on December 27th 2021 with $\alpha = 0.999$.

t^s	t^e	$N^V = 5$	$N^V = 10$	$N^V = 20$	$N^V = 30$	$N^V = 40$	$N^V = 50$
08:00	12:00	1	4	4	11	21	33
08:30	12:30	0	1	3	13	29	37
09:00	13:00	0	1	5	16	26	41
09:30	13:30	0	1	3	5	15	29
10:00	14:00	0	0	0	1	9	23

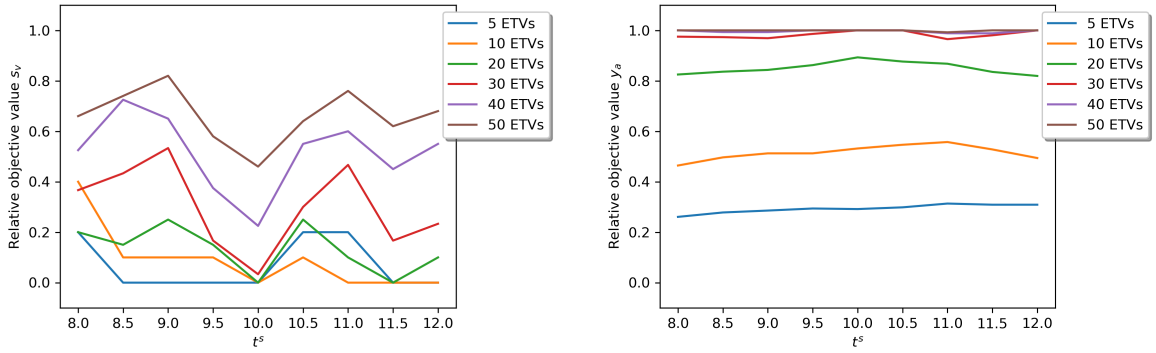

(a) Relative number of unchanged schedules for varying t^s and N^V.

(b) Relative number of aircraft towed for varying t^s and N^V.

Fig. 8 Relative value of unchanged schedules, S/N^V, and aircraft towed, Y/N^F, in the assignments created with the disrupted model ($\alpha = 0.999$), for varying starting times t^s, on December 27th 2021.

V. Sensitivity analysis

In this section, we analyze the performance of the MILP models introduced in Sections II and III when changing certain model parameters or inputs.

A. The impact of fleet size on vehicle-to-aircraft assignments

An important parameter to investigate is the fleet size N^V. If N^V is large enough, all aircraft can be towed by the fleet, i.e. $Y = N^F$. For lower values of N^V, the model has to make a selection from all $a \in A$. In subsequent time periods, the selection of flights will be largely the same, since the goal of the disrupted model is to minimize the number of unchanged schedules. Table 4 and Fig. 8 show the obtained objective values when varying the fleet size. First consider small N^V: observe that for any $\alpha < 1$ the number of towed aircraft is still being maximized. This means any ETV will be assigned many aircraft to tow, with little idle time in between. Therefore, the impact of flight delays on individual towing schedules is large, and Y is small. Now consider N^V large enough so that $Y \approx N^F$. Fig. 8b shows that this is the case for $N^V \geq 30$. Here S/N^V exceeds 0.3, while it does not for smaller N^V. In such an assignment more time is available between towing tasks, leading to a smaller impact of flight delays, and therefore a larger number of towed aircraft. Fig. 8a shows that this not only holds in absolute numbers of S, but also relative to the maxima, i.e. S/N^V.

B. Applying the model to various days of operation

Figure 9 shows the average delay for Schiphol Airport during October 2021 to January 2022. The average of all departure delay averages is 15 minutes, and the average of arrival delay averages is -5 minutes. In addition, the standard deviation is very large. Notable outliers include October 21st 2021 and January 31st 2022, when traffic was disrupted due to weather circumstances [34]. An example of a period with extended large delays is May and June 2022, when Schiphol experienced staff capacity problems. During these months the average departure delay was 31 minutes, and the

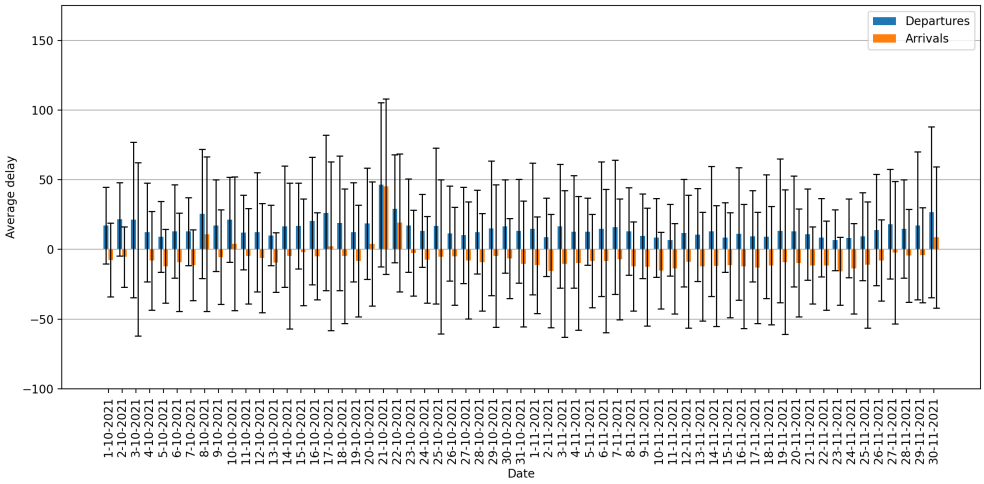

(a) Average daily delay for dates in October and November 2021.

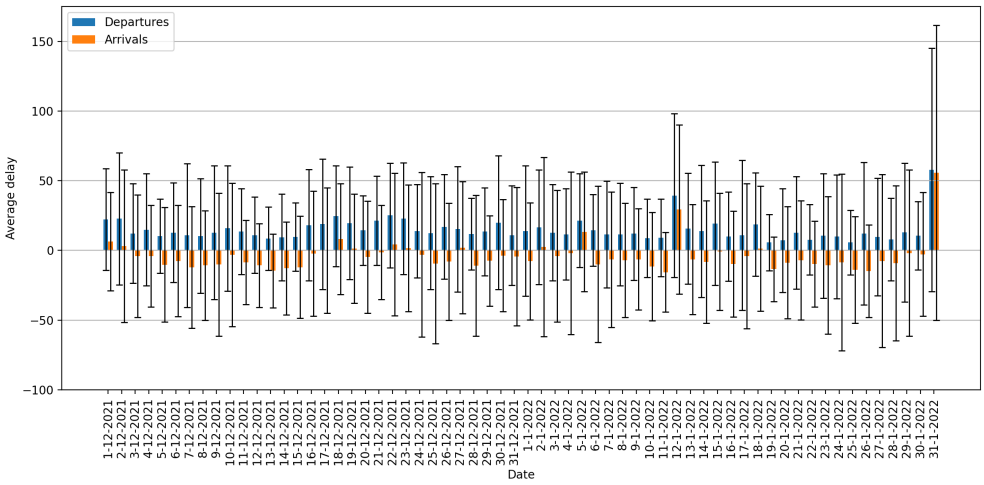

(b) Average daily delay for dates in December 2021 and January 2022.

Fig. 9 Average daily departure and arrival delay including standard deviation for Amsterdam Airport Schiphol during October 2021 to January 2022.

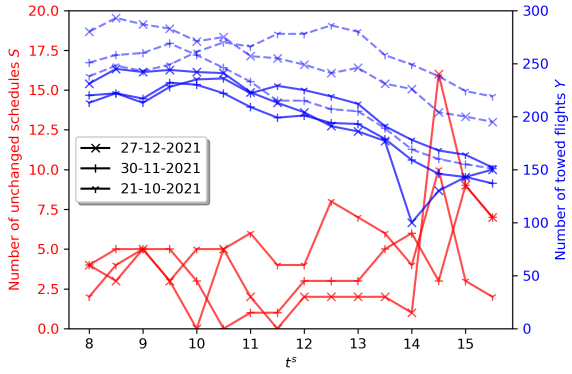

(a) Results of applying the disrupted model to three days. The red solid lines represent the values for S, the blue solid lines the values for Y, and the blue dashed lines the values for N^F.

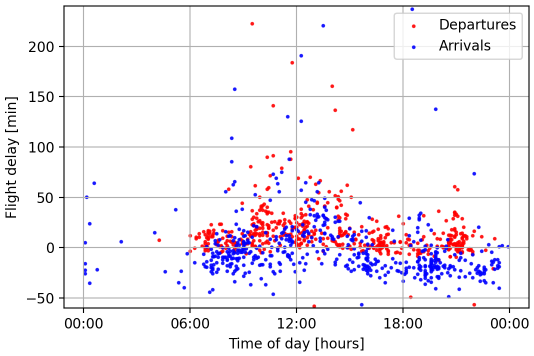

(b) Scatter plot of departure and arrival delays on December 27th 2021.

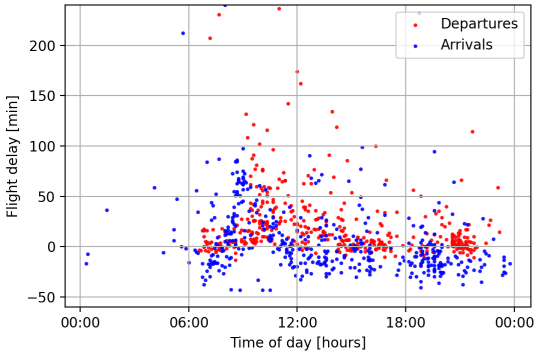

(c) Scatter plot of departure and arrival delays on November 30th 2021.

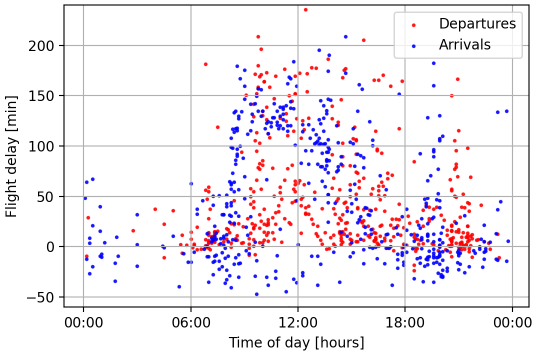

(d) Scatter plot of departure and arrival delays on October 21st 2021.

Fig. 10 Outcomes of applying the disrupted model for three days with varying degrees of on-time performance using $N^V = 20$ at Amsterdam Airport Schiphol, including scatter plots of delays.

average arrival delay was 9 minutes.

In order to investigate how the results are affected if the model is faced with more and greater delays, we compare the results of applying the disrupted model with 20 ETVs for December 27th 2021 (departure delay 15 minutes, arrival delay 2 minutes), to November 30th 2021 (departure delay 27 minutes, arrival delay 9 minutes), and October 21st 2021 (departure delay 47 minutes, arrival delay 45 minutes). In Fig. 10a the metrics for these days are visualized. The figure includes the values obtained for S and Y, as well as those for N^F, i.e. the maximum value for Y. From Fig.10a we note that on November 30th, there were significantly fewer aircraft to tow than on the other days, which means that 20 vehicles is almost enough to tow all aircraft in this case. However, this does not lead to an improved performance in the value of S. Another observation is that a sharp decrease in Y, such as at t^s =14:00 on December 27th, allows for a larger value of S in subsequent time periods. This corresponds to intuition: when the towing assignment becomes relatively empty, there is more space to accommodate flight delays.

Last, an important observation to take from Fig.10a is that there is no clear decrease in performance regarding S when the average flight delays of a day is larger. On October 21st there are roughly as many aircraft to tow as on December 27th, but the average delay is much larger. Still, the number of unchanged schedules obtained with the disrupted model is similar throughout the morning and afternoon. Figures 10b to 10d provide a more detailed illustration of the delays on the tested days. It is clear that especially on October 21st, there are many more large delays than on December 27th.

A possible explanation for this difference in delays, but similarity in the value of S, is the following: delays are assumed to become available to the model when the scheduled flight time is less than half an hour away. This holds for large and small delays. This means that both large and small delays impact the vehicle-to-aircraft assignment in a similar way. Only for very small delays the aircraft will not have to be moved out of its current place in the assignment. For this reason, the model performs similar regardless of the severity of the delays.

VI. Conclusion

This paper proposes an approach to disruption management for the assignment of electric taxiing vehicles to aircraft. First, a strategic MILP model was formulated, which outputs the vehicle-to-aircraft assignment including the state of charge of each vehicle. Second, a disrupted MILP model was introduced, which takes into account the flight delays of the coming half hour when generating its disrupted assignment. By running the disrupted model in staggered time periods, one creates an adaptive vehicle-to-aircraft assignment throughout the day. Both models take the flight schedule and airport layout as inputs, which are used to calculated the vehicle and aircraft routes, for which conflict avoidance is ensured. Both models keep track of the energy spent and gained by the ETVs, and select the times the vehicles are to be charged.

The models are illustrated using a case study of Amsterdam Airport Schiphol. The models are shown to be able to generate vehicle-to-aircraft assignments that correspond to the flight schedules of this hub airport, which include departing and arriving flights that are towed from the gate area to one of the five runways and vice versa. The results show that it is possible to minimize the number of changed schedules, without having to reduce the number of aircraft from the flight schedule that are towed by an ETV, which is beneficial for ETV operators. Furthermore, sensitivity analysis has revealed that the severity of the delays does not impact the model performance, and that if enough ETVs are available to tow all aircraft in the schedule, the number of unchanged schedules increases above 30% of the fleet size.

Future work can include implementing a more detailed routing and energy model within the introduced models by including for example acceleration of aircraft and vehicles, rather than constant velocities. Furthermore, the approach presented in this paper can be tested in combination with varying charging strategies, for example: a strategy where night charging is not preferred, and the ETVs should sustain their state of charge throughout the day.

Acknowledgments

This research was partly funded by the European Regional Development Fund (ERDF) with Grant No. KVW-00235.

References

[1] Federal Aviation Administration, "Aviation Climate Action Plan," , 2021. URL https://www.faa.gov/sites/faa.gov/files/2021-11/Aviation{_}Climate{_}Action{_}Plan.pdf.

[2] IATA, "Net-Zero Carbon Emissions by 2050," , 2021. URL https://www.iata.org/en/pressroom/2021-releases/2021-10-04-03/.

[3] Camilleri, R., and Batra, A., "Assessing the environmental impact of aircraft taxiing technologies," *32nd Congress of the International Council of the Aeronautical Sciences, ICAS 2021*, , No. September, 2021.

[4] Deonandan, I., and Balakrishnan, H., "Evaluation of strategies for reducing taxi-out emissions at airports," *10th AIAA Aviation Technology, Integration and Operations (ATIO) Conference*, Vol. 3, 2010. https://doi.org/10.2514/6.2010-9370.

[5] Schiphol, "The benefits of sustainable taxiing," , 2021. URL https://www.schiphol.nl/en/innovation/page/the-benefits-of-sustainable-taxiing/.

[6] Hospodka, J., "Cost-benefit analysis of electric taxi systems for aircraft," *Journal of Air Transport Management*, Vol. 39, 2014, pp. 81–88. https://doi.org/10.1016/j.jairtraman.2014.05.002, URL http://dx.doi.org/10.1016/j.jairtraman.2014.05.002.

[7] Vaishnav, P., "Costs and benefits of reducing fuel burn and emissions from taxiing aircraft," *Transportation Research Record*, 2014, pp. 65–77. https://doi.org/10.3141/2400-08.

[8] Roling, P., Sillekens, P., and Curran, R., "The effects of electric taxi systems on airport surface congestion," *15th AIAA Aviation Technology, Integration, and Operations Conference*, 2015, pp. 1–10. https://doi.org/10.2514/6.2015-2592.

[9] Khammash, L., Mantecchini, L., and Reis, V., "Micro-simulation of airport taxiing procedures to improve operation sustainability: Application of semi-robotic towing tractor," *5th IEEE International Conference on Models and Technologies for Intelligent Transportation Systems (MT-ITS)*, 2017, pp. 616–621. https://doi.org/10.1109/MTITS.2017.8005587.

[10] Guo, R., Zhang, Y., and Wang, Q., "Comparison of emerging ground propulsion systems for electrified aircraft taxi operations," *Transportation Research Part C: Emerging Technologies*, Vol. 44, 2014, pp. 98–109. https://doi.org/10.1016/j.trc.2014.03.006, URL http://dx.doi.org/10.1016/j.trc.2014.03.006.

[11] Hein, K., and Baumann, S., "Acoustical comparison of conventional taxiing and dispatch towing - Taxibot's contribution to ground noise abatement," *30th Congress of the International Council of the Aeronautical Sciences (ICAS)*, 2016, pp. 1–7.

[12] Lukic, M., Giangrande, P., Hebala, A., Nuzzo, S., and Galea, M., "Review, Challenges, and Future Developments of Electric Taxiing Systems," *IEEE Transactions on Transportation Electrification*, Vol. 5, No. 4, 2019, pp. 1441–1457. https://doi.org/10.1109/TTE.2019.2956862.

[13] van Baaren, E., and Roling, P. C., "Design of a zero emission aircraft towing system," *AIAA AVIATION Forum*, 2019, pp. 1–11. https://doi.org/10.2514/6.2019-2932.

[14] Soltani, M., Ahmadi, S., Akgunduz, A., and Bhuiyan, N., "An eco-friendly aircraft taxiing approach with collision and conflict avoidance," *Transportation Research Part C: Emerging Technologies*, Vol. 121, No. December 2019, 2020, p. 102872. https://doi.org/10.1016/j.trc.2020.102872, URL https://doi.org/10.1016/j.trc.2020.102872.

[15] Ahmadi, S., "Green Airport Operations: Conflict And Collision Free Taxiing Using Electric Powered Towing Alternatives," Ph.D. thesis, 2019.

[16] van Oosterom, S. J., Mitici, M., and Hoekstra, J. M., "Analyzing the impact of battery capacity and charging protocols on the dispatchment of electric towing vehicles at a large airport." *AIAA AVIATION 2022 Forum*, 2022. https://doi.org/https://doi.org/10.2514/6.2022-3920.

[17] Zaninotto, S., Gauci, J., Farrugia, G., and Debattista, J., "Design of a Human-in-the-Loop Aircraft Taxi Optimisation System Using Autonomous Tow Trucks," *AIAA AVIATION Forum*, 2019, pp. 1–13. https://doi.org/10.2514/6.2019-2931.

[18] Salihu, A. L., Lloyd, S. M., and Akgunduz, A., "Electrification of airport taxiway operations: A simulation framework for analyzing congestion and cost," *Transportation Research Part D: Transport and Environment*, Vol. 97, No. July, 2021. https://doi.org/10.1016/j.trd.2021.102962, URL https://doi.org/10.1016/j.trd.2021.102962.

[19] Lee, J., Marla, L., and Jacquillat, A., "Dynamic Airline Disruption Management Under Airport Operating Uncertainty," *SSRN Electronic Journal*, , No. February, 2018. https://doi.org/10.2139/ssrn.3082518.

[20] Lee, J., Marla, L., and Jacquillat, A., "Dynamic Disruption Management in Airline Networks Under Airport Operating Uncertainty," *Transportation Science*, Vol. 54, No. 4, 2020, pp. 973–997. https://doi.org/10.1287/trsc.2020.0983.

[21] Amsterdam Airport Schiphol, "Download a map: aircraft process maps," , 2021. URL https://www.schiphol.nl/en/operations/page/maps/.

[22] Schiphol, "What is sustainable taxiing? (Part 1)," , 2021. URL https://www.schiphol.nl/en/innovation/page/what-is-sustainable-taxiing-part-1/.

[23] Zaninotto, S., Gauci, J., and Zammit, B., "A Testbed for Performance Analysis of Algorithms for Engineless Taxiing with Autonomous Tow Trucks," *AIAA/IEEE Digital Avionics Systems Conference*, Vol. October, IEEE, 2021. https://doi.org/10.1109/DASC52595.2021.9594411.

[24] Roling, P. C., and Visser, H. G., "Optimal Airport Surface Traffic Planning Using Mixed-Integer Linear Programming," *International Journal of Aerospace Engineering*, 2008, pp. 1–11. https://doi.org/10.1155/2008/732828.

[25] Daidzic, N. E., "Determination of taxiing resistances for transport category airplane tractive propulsion," *Advances in Aircraft and Spacecraft Science*, Vol. 4, No. 6, 2017, pp. 651–677. https://doi.org/10.12989/aas.2017.4.6.651.

[26] Schiphol Group, "Schiphol Developer Center," , 2022. URL https://developer.schiphol.nl/login.

[27] Luchtverkeersleiding Nederland, "Runway use," , 2022. URL https://en.lvnl.nl/environment/runway-use.

[28] Dutch Plane Spotters, "Schiphol Runway Usage," , 2022. URL https://www.dutchplanespotters.nl/runways/.

[29] Schiphol, "Schiphol Regulations," Tech. rep., 2022. URL https://www.schiphol.nl/en/download/1609745377/43q9kGoE92CccmEeC6awa4.pdf.

[30] Munich International Airport, "Traffic and Safety Rules: for the non-public area at Munich Airport," Tech. rep., Munich International Airport, 2016. URL https://www.munich-airport.de/{_}b/0000000000000008368639bb5e302e6f/traffic-safety-rules-2016.pdf.

[31] Smart Airport Systems, "Taxibot International," , 2022. URL https://www.taxibot-international.com/.

[32] Schiphol, "Sustainable taxiing and the Taxibot," , 2020. URL https://www.schiphol.nl/en/download/b2b/1594319068/40LYaERw5x8BuRuXpVQkiK.pdf.

[33] Adegbohun, F., von Jouanne, A., and Lee, K. Y., "Autonomous battery swapping system and methodologies of electric vehicles," *Energies*, Vol. 12, No. 4, 2019, pp. 1–14. https://doi.org/10.3390/en12040667.

[34] Amsterdam Airport Schiphol, "Possible delays and cancellations due to strong wind," , 2021. URL https://www.schiphol.nl/en/messages/possible-delays-and-cancellations-due-to-strong-wind.